13 Identifying and Assessing Critical Uncertainty Thresholds in a Forest Pest Risk Model

Frank H. Koch[1]* and Denys Yemshanov[2]

[1]*USDA Forest Service, Southern Research Station, Eastern Forest Environmental Threat Assessment Center, Research Triangle Park, North Carolina, USA;* [2]*Natural Resources Canada, Canadian Forest Service, Great Lakes Forestry Centre, Sault Ste. Marie, Ontario, Canada*

Abstract

Pest risk maps can provide helpful decision support for invasive alien species management, but often fail to address adequately the uncertainty associated with their predicted risk values. This chapter explores how increased uncertainty in a risk model's numeric assumptions (i.e. its principal parameters) might affect the resulting risk map. We used a spatial stochastic model, integrating components for entry, establishment and spread, to estimate the risks of invasion and their variation across a two-dimensional gridded landscape for *Sirex noctilio*, a non-native woodwasp detected in eastern North America in 2004. Historically, *S. noctilio* has been a major pest of pine (*Pinus* spp.) plantations in the southern hemisphere. We present a sensitivity analysis of the mapped risk estimates to variation in six key model parameters: (i) the annual probabilities of new *S. noctilio* entries at US and Canadian ports; (ii) the *S. noctilio* population-carrying capacity at a given location; (iii) the maximum annual spread distance; (iv) the probability of local dispersal (i.e. at a distance of 1 km); (v) the susceptibility of the host resource; and (vi) the growth rate of the host trees. We used Monte Carlo simulation to sample values from symmetric uniform distributions defined by a series of nested variability bounds around each parameter's initial values (i.e. ±5%, ..., ±50%). The results show that maximum annual spread distance, which governs long-distance dispersal, was the most sensitive of the tested parameters. At ±15% uncertainty in this parameter, mapped risk values shifted notably. No other parameter had a major effect, even at wider bounds of variation. The methods presented in this chapter are generic and can be used to assess the impact of uncertainties on the stability of pest risk maps or to identify any geographic areas for which management decisions can be made confidently, regardless of uncertainty.

Introduction to Uncertainty Analysis

This chapter describes methods for analysing uncertainty in key parameters of a spatial stochastic model used to estimate invasion risk. The model was applied to forecast the likely geographic pattern of invasion of a recently arrived forest pest, the sirex woodwasp (*Sirex noctilio* Fabricius), in eastern North America (Yemshanov *et al*., 2009a). One primary benefit of a spatial

* Corresponding author. E-mail: fhkoch@fs.fed.us

 Pest Risk Modelling and Mapping for Invasive Alien Species (ed. R.C. Venette)

stochastic modelling approach is that the various stages of an invasion – its arrival, spread and establishment components – can be depicted within a single modelling framework (Yemshanov *et al*., 2009c). Unlike other risk modelling methods that focus only on a single stage of invasion (e.g. environmental niche models, which are aimed primarily at characterizing risk of successful establishment), the approach is relatively data-intensive; in particular, it requires estimation of aspects of a pest's population or meta-population dynamics, its host distribution and its general dispersal behaviour. Nonetheless, by adopting an approach of repeated stochastic model simulations, it is possible to quantify the risk of invasion as a numeric probability (Rossi *et al*., 1993; Rafoss, 2003) for each geographic location (i.e. map cell) comprising the model's spatial domain (i.e. the study area). The approach also allows one to calculate the variation of the risk estimates. Thus, spatial stochastic simulation provides, for each geographic location, an estimate of both the invasion risk and the uncertainty associated with that risk estimate (Yemshanov *et al*., 2009a). In this case, uncertainty is synonymous with variability in model inputs (i.e. parametric uncertainty) and outputs. Uncertainties resulting from the use of imprecise terms or lack of knowledge are not addressed explicitly.

Importantly, the uncertainties associated with model outputs represent cumulative measures of uncertainties that may arise from a variety of sources; in particular, uncertainty associated with a model's parameters, its input data and possibly its structure or formulation may all contribute to the output uncertainty (Elith *et al*., 2002; Regan *et al*., 2002; Walker *et al*., 2003; Refsgaard *et al*., 2007). Additional analytical techniques are necessary to explore how uncertainty in any of these particular model elements might be influencing the outputs. The focus of this chapter is on a practical approach, first outlined in Koch *et al*. (2009), to examine specifically the impact of model parametric uncertainty. We use a Monte Carlo simulation approach to sensitivity analysis to do this. Monte Carlo methods involve repeated random sampling from a range of possible input values (e.g. from a probability distribution associated with a model parameter). When model simulations are completed with these randomly sampled input values, the simulation results can be compiled to obtain estimates of a phenomenon of interest.

The primary objective of sensitivity analysis in this context is to determine the relative contribution of individual model parameters to the uncertainty in the resulting outputs (Helton *et al*., 2006). The application of sensitivity analysis to analysing parametric uncertainty is not novel (Morgan and Henrion, 1990; Li and Wu, 2006). What makes our analysis unique is that it is applied in a spatial domain. The analysis of uncertainty is uncommon in risk maps, probably because of the perceived difficulty (Morgan and Henrion, 1990; Andrews *et al*., 2004; Cook *et al*., 2007). However, we believe that it is critical because invasions are spatial, or more precisely, spatiotemporal, processes and so it is logical to analyse the associated uncertainties from a map-based perspective.

A variety of mathematical, statistical and graphical methods have been utilized for sensitivity analysis (Frey and Patil, 2002). For a spatial stochastic model such as ours, with its capacity to generate many different realizations of the invasion process, a basic Monte Carlo approach offers a straightforward way to examine model parameter sensitivities. We begin by performing repeated simulations with the invasion model in order to get a mapped set of risk estimates based on the parameters' initial values (i.e. based on our best estimates for these values, which we determined either analytically or by consulting experts prior to running the model). The resulting set of risk estimates constitutes a baseline scenario for later comparison to the sensitivity analysis results. Because the model is stochastic, the baseline estimate for each map cell includes both the primary risk metric, P, which is a numeric probability indicating the proportion of simulation

runs where successful invasion occurs, and a measure of uncertainty in that estimate, $\sigma(P)$, the standard deviation of P. Next, we identify key model parameters and vary their values within a specified set of nested bounds (±5%, ±10%, ..., ±50%), which alters the pattern of output variation. Using these nested bounds, we complete many additional simulation runs so that we can compare the parameters with one another in terms of the relative impact of uncertainty (e.g. which parameters are most sensitive at ±15% variation in their baseline values).

The analytical approach has three main objectives: (i) to identify any parameters that are highly influential and thus should be thoroughly scrutinized with respect to the consequences of uncertainty; (ii) for any influential parameters, to find the level(s) of uncertainty in inputs that dramatically change output maps (i.e. the output risk and uncertainty estimates) and so affect the maps' utility for end users (i.e. decision makers); and (iii) to determine if, even with added uncertainty, any portions of an output map remain stable enough in the presence of parametric uncertainty for an end user to utilize the map for decision support, regardless of the uncertainty.

Sensitivity analysis has a few important limitations. For instance, as applied, the approach does not address sources of uncertainty in the input data (i.e. the spatial uncertainty in particular), although a similar Monte Carlo approach can be used to vary input data for the purposes of sensitivity/uncertainty analysis (Crosetto *et al*., 2000; Crosetto and Tarantola, 2001). In theory, Monte Carlo techniques could also be used to compare the sensitivity of different model formulations (i.e. model formulation uncertainty) but would require significant time for computations.

Furthermore, Monte Carlo sensitivity analysis does not deal well with severe uncertainty. For models involving invasive alien species, especially recently discovered invaders, large empirical knowledge gaps may exist regarding the most important invasion drivers. This lack of knowledge makes it difficult to identify meaningful bounds in which to vary parameter values. In our case, we used a hierarchical set of percentage bounds (up to ±50%) around the values of the parameters we analysed, but in theory a parameter (e.g. the annual probability of new entries) may be off by a factor of 100, 1000 or more. Consequently, the analytical approach described here should be seen only as a local or restricted analysis of parametric uncertainty. We believe it is appropriate for the pest highlighted in this chapter (*S. noctilio* Fabricius) because the biology and behaviour of *S. noctilio* have been reasonably well documented in portions of both its native and invaded ranges. Other analytical frameworks, such as info-gap decision theory (Ben-Haim, 2006), may be better for severe parametric uncertainty.

Monte Carlo sensitivity analysis also assumes that the correct parameters to include in the model and for which to perform sensitivity/uncertainty analysis have been identified. If a model is missing key parameters or includes unnecessary or deleterious parameters, the accuracy of the output risk estimates is likely to be affected. These inaccuracies are most likely to be revealed during some sort of validation or cross-validation process with empirical data. Such data are often hard to acquire for invasive alien species. However, whether the correct set of parameters has been included in a model is really a question of model formulation uncertainty.

Because the model described in this chapter was implemented as a risk forecasting approach with essentially no opportunity for validation (i.e. *S. noctilio* was not widely distributed in North America when we performed this work), the sensitivity analysis results should be interpreted only as an assessment of the relative, and not absolute, relationships between model parameters and outputs. This is a critical point: the approach does not address the accuracy of the risk predictions, but does allow the analyst to get a basic sense of the robustness of model outputs to parametric uncertainty. Thus, while we cannot always verify or validate the accuracy of a given risk model, we can determine whether model results have any

reliable decision-making value in the face of uncertainty. For instance, the technique described here allows us to identify influential parameters and, just as importantly, determine when uncertainty in a parameter starts to have a significant impact on the output risk estimates (i.e. changes a risk estimate from a relatively high value to a comparatively lower value).

Case Study: Invasion of *S. noctilio*

We modelled the potential invasion of the woodwasp species *S. noctilio* in eastern North American forests. Native to Europe, western Asia and northern Africa, *S. noctilio* has been introduced in many parts of the world and is considered an important pest of pine (*Pinus* spp.) plantations in the southern hemisphere (Carnegie *et al*., 2006; Corley *et al*., 2007). The insect has particularly impacted plantations in eastern Australia, New Zealand, South Africa and several South American countries including Brazil, Chile and Argentina. Given the insect's wide bioclimatic tolerance (Carnegie *et al*., 2006) and an abundance of potential hosts, *S. noctilio* was viewed as a major invasion threat to North America for several years before it was found in upstate New York in 2004 (Hoebeke *et al*., 2005) and southern Ontario in 2005 (de Groot *et al*., 2006). Essentially, it is expected to persist throughout temperate pine forests of the USA and southern Canada, although it may require 2 or 3 years to complete a generation at higher latitudes (i.e. cooler climates; Borchert *et al*., 2007). Pine density in the initially invaded region is comparatively low; as a result, the pest might find greater success were it to spread into the southern USA.

At the time of our analysis, *S. noctilio* had been found in more than 20 counties in New York, several counties in north-central Pennsylvania, and individual counties in Michigan and Vermont. The woodwasp had also been discovered throughout much of southern Ontario. Since that time, this insect has been discovered in additional counties in the states named above, as well as one county each in Ohio, New Jersey and Connecticut, and in western Quebec (National Agricultural Pest Information System, 2013).

With respect to hosts, *S. noctilio* has caused the greatest impacts in plantations of loblolly (*Pinus taeda*) and Monterey pine (*Pinus radiata*) in the southern hemisphere. In North America, *S. noctilio* has been confirmed as a pest on several native pines: red pine (*Pinus resinosa*), eastern white pine (*Pinus strobus*) and jack pine (*Pinus banksiana*) (Dodds *et al*., 2007). This insect is also found on Scots pine (*Pinus sylvestris*) in managed and unmanaged Christmas tree farms (Dodds *et al*., 2010). Scots pine is known as a host in the pest's native region. Evidence suggests that a number of pine species in eastern North America are suitable, if not preferred hosts. The geographic distributions of these pine species overlap and facilitate the natural spread of the insect.

S. noctilio can disperse naturally by adult flight or through human activities (e.g. movement of infested logs). It is generally known as a strong flier, but few empirical studies have been performed to quantify its dispersal capabilities (but see Corley *et al*., 2007). Regardless, the initial introduction of *S. noctilio* into North America was almost certainly human-mediated, likely in raw wood or solid-wood packing materials associated with international trade (Hoebeke *et al*., 2005).

Model and Data Sources

We used a spatially explicit, raster-based modelling framework to perform the simulations for this study. As a dynamic spatiotemporal model (Gibson and Austin, 1996; Fuentes and Kuperman, 1999), it departs from deterministic risk modelling approaches, which typically adopt the simplifying assumption that an invader's potential distribution is already in equilibrium with its environment.

The model was programmed in C++. Although the model code is not available for public use, the uncertainty analysis techniques described in this chapter can be

applied to any spatial stochastic model with a similar structure. The primary requirement is that each model run yields a binary map that documents the absence (0) or occurrence (1) of some event. In our case, we simulated the annual spread and survival of *S. noctilio* over 30 years, such that each simulation run yielded a binary raster map indicating where in eastern North America the insect would have viable populations at the end of the specified time horizon. These maps are then compiled to compute a numeric probability of the event (i.e. for each map location, j, the proportion of model runs in which the event occurred, P_j) and the associated uncertainty (i.e. standard deviation of P_j, $\sigma(P_j)$) for each map location (i.e. each raster map cell). Each grid cell in the model was 5 km × 5 km, which we selected for practicality. The coarser resolution allowed us to reduce the computation time for individual simulation runs, a large number of which were necessary to analyse a set of sensitivity analysis scenarios.

In general terms, the model simulates forest growth, new arrivals, spread and survival of *S. noctilio* across eastern North America in discrete time steps (Yemshanov *et al*., 2009b). The model is simple with limited data requirements. Some model elements, particularly those related to dispersal, were developed from expert knowledge because empirical data were unavailable. We believe this limitation is common for many invasive alien species. For advice about eliciting expert estimates in lieu of data and then incorporating them into a model, see Morgan and Henrion (1990) and Yamada *et al*. (2003).

The model simulates three events for *S. noctilio*: (i) new arrivals at US and Canadian ports; (ii) spread across eastern North America; and (iii) establishment in suitable locations. Details for these simulations appear in the online supplement to Chapter 13. Additionally, Table 13.1 provides a brief summary of the main parameters and their roles within the model. Notably, we performed sensitivity analyses only for six model parameters: (i) $W_{x(t)}$, the annual probabilities of new local entries of *S. noctilio* at individual US and Canadian ports; (ii) $d_{\max}$, the maximum annual spread distance; (iii) p_0, the local dispersal probability; (iv) s_v, the susceptibility of the host resource; (v) k, the carrying capacity for a population of *S. noctilio* at a given location; and (vi) g_v, the growth rate of the host trees. We chose this particular subset of parameters after initial model testing to limit computation time. The sensitivity analysis approach described here could certainly be applied to all of a model's parameters, but we felt total analysis was unnecessary to demonstrate the methodology. Furthermore, many models include parameters that are related to or dependent on one another in some way. For the sake of computational efficiency, it may make sense to choose one representative parameter out of related sets of parameters. However, this choice may only be practical if the analyst is familiar with a model's structure and outputs.

Although we used C++ for model development, similar models could be created in a software package like R or MATLAB that can accommodate spatial data. Both of these packages can store the map data as matrices and can implement basic statistical, mathematical and stochastic functions (e.g. testing model-derived probabilities against values from a uniform random distribution). The biggest constraint is likely to be computation time; packages like R are unlikely to be as computationally efficient as optimized code in C++, Java or similar programming languages. Because of the large number of simulation runs required for this sort of exercise, spreadsheet-based Monte Carlo software packages, such as @RISK or CRYSTAL BALL, would probably be unsuitable except at very coarse spatial scales or for small spatial areas.

Analyses

Baseline scenario

We initially used the model for a baseline scenario of *S. noctilio* spread in eastern North America over a 30-year time horizon (from 2006 to 2036). Under this baseline scenario,

Table 13.1. Parameters for components of the *Sirex noctilio* invasion model. The six parameters tested via sensitivity analysis are highlighted in bold.

Parameter	Description
All components	
t	Annual time step for the model
T	30-year time horizon for summarizing the model results (2006–2036)
New arrivals	
t_0	Used in calculating $F(t)$; corresponds to earliest year for which summary import data were available for the USA and Canada
T_{entry}	Used in calculating $F(t)$; corresponds to the presumed year that *S. noctilio* arrived in eastern North America
$F(t)$	Function describing the yearly flow of marine imports to the USA and Canada through time
$p(t)$	Total probability of successful *S. noctilio* entry into North America in year t; derived from $F(t)$
x	Individual port of entry that receives commodities associated with *S. noctilio*; total number of ports = 148
$v_{x(t)}$ ($V_{x(t)}$)	Tonnage of *S. noctilio*-associated cargo received at port x in year t; converted to a proportion, $V_{x(t)}$, of the total *S. noctilio* tonnage for the region that was received at that particular port x
$\boldsymbol{W_{x(t)}}$	Vector of the local probabilities of *S. noctilio* entry at each port x in year t; derived from $V_{x(t)}$
Spread	
$b(d)$	Colonization rate (i.e. rate of successful dispersal) as a function of the distance, d, from the nearest location with an established *S. noctilio* population; influenced by p_0 and d_{max}
$\boldsymbol{p_0}$	Local dispersal probability (i.e. probability of dispersal at a distance of 1 km)
$\boldsymbol{d_{max}}$	Maximum distance at which dispersing *S. noctilio* populations become established
Establishment	
$N_{j(t)}$; $N_{j(t+1)}$	*S. noctilio* population densities in grid cell j at years t and $t + 1$
R	Annual *S. noctilio* population growth rate
$\boldsymbol{k}$	Carrying capacity that constrains maximum population size
$_{j(t)}$	Maximum volume of pine killed by *S. noctilio* in year t; depends on μ
μ	Minimum volume of pine required to support a single population unit
$\boldsymbol{g_v}$	Function describing the age-dependent rate of host (pine) stand growth
$\boldsymbol{s_v}$	Function describing the age- and species-dependent level of host (pine) susceptibility; influenced by a_j, a_0, a_{max} and s_{max}
a_j	Host stand age in years (i.e. the average stand age in a map cell)
a_0	Age of host stand closure (20 years)
a_{max}	Age when host stand reaches its maximum level of susceptibility
s_{max}	Maximum susceptibility value for ageing host stands

Please see the online supplement to Chapter 13 for more information about the model components.

model parameter values were left as originally specified during model development (i.e. as determined analytically or from expert estimates; see the online supplement to Chapter 13 for additional details). We initialized the model with a map of known *S. noctilio* infestations as of 2006, the first year when systematic field detection surveys were performed in the USA and Canada.

We generated two output metrics for this baseline scenario that we also utilized in our subsequent sensitivity analyses. The first was P_j, the probability that *S. noctilio* invades map cell j at the end of the forecast horizon. This served as our primary metric of invasion risk. The value of P_j for each map cell was calculated from the repeated model simulations:

$$P_j = \frac{\sum_{u=1}^{U} \tau_{j,u,T}}{U} \quad (13.1)$$

where $\tau_{j,u,T}$ is a binary variable indicating presence or absence of *S. noctilio* in cell *j* at time horizon *T* for a single model replication *u* and *U* is the total number of replications for the scenario. Less than 500 replications were required for the baseline scenario to stabilize (see subsection 'Sensitivity analysis scenarios' below for further discussion about stabilization). In addition, the variation of the P_j values was characterized with a map of $\sigma(P_j)$, the standard deviation of *P* for each cell, which was our primary metric of the output uncertainty. The standard deviation is a commonly used metric of the uncertainty in an estimate, but it has some limitations, perhaps most notably that it can be sensitive to extreme observations. We adopted $\sigma(P_j)$ as our uncertainty metric for the sake of computational simplicity, but other uncertainty metrics such as binary entropy (MacKay, 2003) could be applied in the analyses described here.

From the maps we generated for the baseline scenario (Fig. 13.1; see colour plate section), we can make several broad forecasts regarding the expected path of the *S. noctilio* invasion in eastern North America. First, the risk of invasion (i.e. P_j; Fig. 13.1a) is expected to be high ($P_j > 0.75$) throughout the north-eastern USA, southern Ontario and Quebec, which is unsurprising because the pest is already established in this region. The area of relatively high risk also extends into the northern portion of the south-eastern USA; indeed, the southern edge of the main invasion front is expected to be near the Virginia–North Carolina border and the western edge along the eastern shore of Lake Superior in 2036. Output uncertainty (i.e. $\sigma(P_j)$; Fig. 13.1b) is generally highest near this predicted main front. Beyond the main front, the south-eastern USA contains extensive areas of medium-level ($0.25 \leq P_j \leq 0.75$) risk near the Atlantic and Gulf coasts (i.e. near possible ports of entry). Notably, this region contains large areas of pine forest, most of which is dominated by loblolly pine, a species understood to be highly susceptible to *S. noctilio* (see Table S13.3 in the online supplement to Chapter 13). The output uncertainty tends to be high here because the probability of a new *S. noctilio* entry at any port, and its subsequent spread and establishment, is relatively moderate compared with the probability of expansion in northern areas near existing infestations. Notably, areas of the south-eastern USA that are further inland (i.e. non-coastal) exhibit both low risk and low uncertainty, which reflects less abundant hosts and greater distance from possible sources of invaders, either ports of entry or the advancing main front.

Sensitivity analysis scenarios

We analysed the sensitivity of the invasion risk estimates using a Monte Carlo approach with four general steps: (i) defining a probability distribution for each parameter of interest; (ii) sampling from this distribution to select a value; (iii) running multiple simulations of the risk model with the parameter values sampled from the distributions; and (iv) summarizing the results from repeated realizations of this process. As acknowledged earlier, a parameter may be poorly specified due to lack of data, so its associated distribution may have to be approximated. In some cases, information about the parameter may be insufficient to characterize even the primary moments (i.e. the mean and variance) of a probability distribution. In other cases, a parameter's empirical distribution may be reasonably well fit by one of the many commonly used theoretical distribution functions (e.g. the normal, exponential or Cauchy distributions). Regardless, a simpler solution may be to assume a uniform distribution for each parameter (Morgan and Henrion, 1990). In our case, we employed a nested set of variability bounds around each tested parameter: ±5%, ±10% and so on up to ±50%. Each pair of 'plus–minus' bounds defined the end points for a symmetric uniform distribution from which we sampled values randomly. A benefit of

applying the same percentage increments to all parameters (i.e. rather than changing each parameter according to an independent scale) is that comparisons of their degree of sensitivity become more straightforward.

For the sensitivity analysis, we varied one parameter at a time, while leaving all other parameters unchanged. To verify the relative impact of specific parameters, we also used the alternative approach of varying all tested parameters but one, which was kept at the baseline. Because s_v and g_v were represented as tables of values (Table 13.1; online supplement to Chapter 13), when varying either or both of these parameters, all values in the table(s) were altered identically based on the value sampled randomly from the associated uniform distribution. We must emphasize that our sampling choices (i.e. utilizing uniform distributions and sampling in ±5% increments to a maximum of ±50%) were somewhat arbitrary, although informed by our previous experience with initial testing of the model and an awareness of what would be computationally practical. In our case, these particular choices permitted us to perform a fairly comprehensive analysis of parametric uncertainty, but they may not work well for a different model applied to a different pest.

Analysts who intend to complete similar analyses should consider at least two things. First, they should decide if it is reasonable to approximate the distributions of tested parameters with something other than the uniform distribution. Certain statistical tests (e.g. Kolmogorov–Smirnov test, chi-squared test) can help determine whether a set of data are consistent with the normal distribution or some other proposed distribution, but this assumes the data for a parameter of interest are sufficient for valid testing (Morgan and Henrion, 1990). Second, as alluded to earlier in the chapter, the analysts must also identify levels of variation that will yield meaningful and interpretable results regarding the parameter sensitivities. Unfortunately, this can be a lengthy iterative process and may not be possible for species that lack even basic information for parameterizing an invasion model.

Sensitivity tests and metrics

For complex stochastic simulation models, hundreds or even thousands of replications may be necessary to stabilize the outputs (i.e. to minimize the variation in the output values that can arise simply from completing too few replications). This is especially true when a large amount of variability (i.e. uncertainty) is added to model parameters, as was the case in our sensitivity scenarios. One metric that can be used to determine the minimum number of model replications required for output map stability is S_{XY}, the sum of the squared differences in P_j map values between two trials incorporating consecutively increasing numbers of replications:

$$S_{XY} = \sqrt{\sum_{j=1}^{M}\left[\left(P_{jX} - P_{jY}\right)^2\right]} \qquad (13.2)$$

where M is the total number of map cells covering eastern North America (~156,000 cells) and P_{jX} and P_{jY} are the invasion probabilities for map cell j in trials using X and Y number of replications, $X > Y$. When S_{XY} is plotted against the number of replications Y, it depicts a declining curve; when this curve begins to flatten rather than decline, this indicates that the model has stabilized. We found that most of the sensitivity scenarios converged after 2400–2700 replications (Fig. 13.2), so we generated maps of P_j and $\sigma(P_j)$ based on 3000 model replications for each scenario. As Fig. 13.2 also suggests, other metrics, such as the square root of the total map area where P_j or $\sigma(P_j)$ is below some specified threshold, can be used to assess model stability, but they may not be as easily interpretable as S_{XY}. In our case, these latter two metrics both appear as gradually increasing curves, where the flattening that indicates model stability is not as immediately obvious as with the S_{XY} metric (Fig. 13.2).

To evaluate the effect of introduced parametric uncertainty on the output uncertainty of the risk maps (i.e. on the $\sigma(P_j)$ values), we calculated 'uncertainty ratios' for each sensitivity scenario. For any given map cell, the uncertainty ratio is the value of

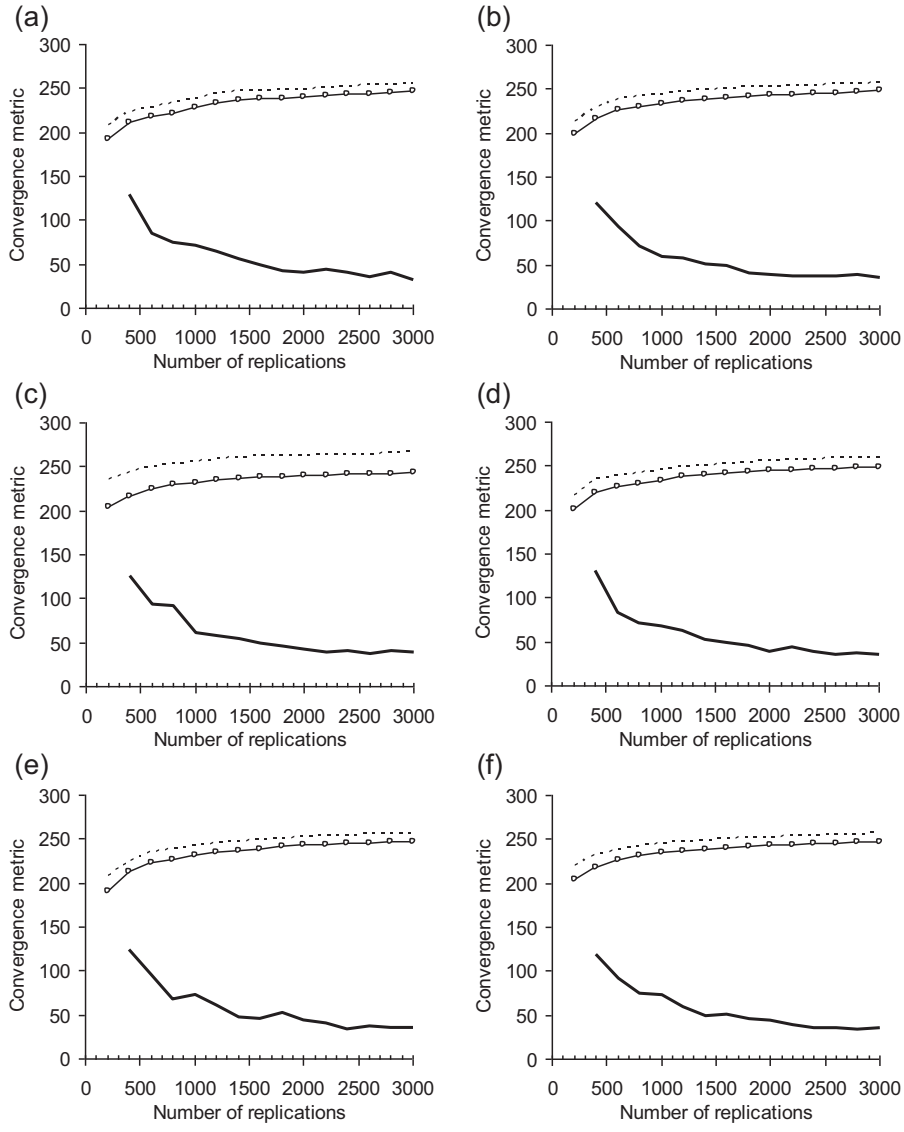

Fig. 13.2. Convergence metric values versus number of replications, at ±40% parametric uncertainty. Tested parameters: (a) local probabilities of entry at marine ports, $W_{x(t)}$; (b) population carrying capacity, k; (c) maximum annual spread distance, d_{max}; (d) local dispersal probability, p_0; (e) host susceptibility, s_v; (f) host growth rate, g_v.

$\sigma(P_j)$ for the scenario of interest divided by $\sigma(P_j')$ for the baseline scenario. An uncertainty ratio value close to 1 indicates that varying the parameter value at the specified level does not substantially change the variability (i.e. uncertainty) of the output risk estimate. Ratio values approaching 0 indicate decreasing uncertainty in the

output risk estimates, while as values progress above 1, they indicate increasing uncertainty in these estimates. Although the uncertainty ratio is a relatively simple metric, it can be mapped such that it enables straightforward visual comparison of the results of the different sensitivity scenarios, even when the compared parameters are widely different in scale or structure.

Visualizations of Uncertainty

Figure 13.3 (see colour plate section) shows uncertainty ratio maps for several of the model parameters at ±40% uncertainty. In the one-parameter-at-a-time sensitivity scenarios, changes to the maximum annual spread distance, d_{max}, increased uncertainty ratios across a large portion of the map area (Fig. 13.3a). In particular, high uncertainty ratios appeared in a broad band just beyond the estimated invasion front and in a few areas inside the front, such as coastal New England. These latter areas exhibited high risk, yet low uncertainty, under the baseline scenario. Changes to the local dispersal probability, p_0 (Fig. 13.3b), also elevated uncertainty ratio values in these locations, but to a lesser degree than observed for d_{max}. Furthermore, unlike for d_{max}, the uncertainty ratios for p_0 were < 1 in the north-western portion of our study area (i.e. the western Great Lakes region). We believe that increased uncertainty in p_0 permitted more invasion nuclei to develop in this remote area through time, which raised the invasion risk estimates, but at the same time stabilized the output uncertainties at a lower level than under the baseline scenario. This phenomenon also occurred with the other parameters besides d_{max}, as exemplified by the ratio map for the port entry probabilities parameter, $W_{x(t)}$ (Fig. 13.3c). Additionally, the map for $W_{x(t)}$ shows another phenomenon we observed for all parameters except d_{max} and p_0: high uncertainty ratios in only a small proportion of the study area, mostly near the edge of the host range (i.e. near the invasion's biological limits).

Essentially, the uncertainty ratio maps for the all-but-one sensitivity scenarios (Fig. 13.3d–f; see colour plate section) show the opposite of the one-at-a-time scenarios. When d_{max} (Fig. 13.3d) was the only parameter left fixed at its baseline value, and all other parameters were varied uniformly within a ±40% bound, the uncertainty ratios were low to moderate throughout most of the study area. In contrast, when any other single parameter was left fixed, such as the population carrying capacity, k (Fig. 13.3e), or the host growth rate, g_v (Fig. 13.3f), the uncertainty ratio values increased substantially across most of the study area. This pattern appears to confirm that d_{max} was the most influential parameter on the model outputs.

Although the uncertainty ratio maps facilitate visual comparison, they do not really quantify the differences between the sensitivity scenarios. It is possible to calculate this difference by using the S_{XY} metric (Eqn 13.2) in a second way: to compare the maps of P_j and $\sigma(P_j)$ for each sensitivity scenario, X, with the matching maps from the baseline scenario, Y. In this case, S_{XY} is calculated as the sum of the cumulative differences between the sensitivity scenario's P_j or $\sigma(P_j)$ map and the corresponding baseline scenario map of P_j or $\sigma(P_j)$. Thus, S_{XY} in this context depicts cumulative changes in the *S. noctilio* risk map due to the introduction of parametric uncertainty.

We cross-tabulated the S_{XY} differences for eastern North America as well as three smaller focus regions: eastern Canada, the north-eastern USA and the south-eastern USA. Figure 13.4 shows the results for all regions at ±25% and ±40% parametric uncertainty. For the entire study area, and whether calculated from the P_j or $\sigma(P_j)$ maps, the cross-tabulation results indicate that d_{max} was by far the most sensitive of the tested model parameters. The graphs of S_{XY} for P_j (Fig. 13.4a and c) suggest that p_0 was the second most-sensitive parameter when considering the entire study area. Both of these observations were also true for eastern Canada and the north-eastern USA. In

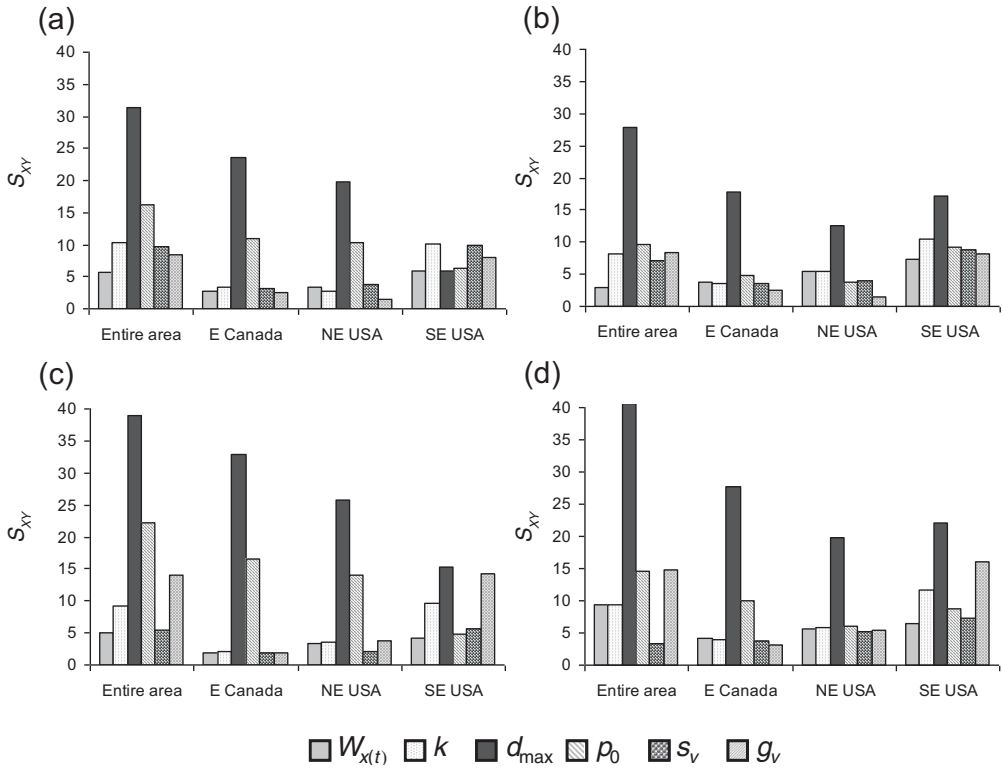

Fig. 13.4. Regional summaries of the S_{XY} metric for the sensitivity analyses. Results from one-parameter-at-a-time sensitivity analyses are presented at two variability increments: (a) for P_j at ±25% parametric uncertainty; (b) for $\sigma(P_j)$ at ±25%; (c) for P_j at ±40%; (d) for $\sigma(P_j)$ at ±40% parametric uncertainty.

contrast, the results for the south-eastern USA suggest relatively less importance for d_{max}, and greater importance for g_v, which was nearly as important as d_{max} at ±40% uncertainty (Fig. 13.4c and d). Indeed, g_v also showed moderately high sensitivity for the entire study area at ±40% uncertainty (Fig. 13.4c and d). We believe this outcome is explained by the fact that the south-eastern US region is host-rich but relatively far from currently infested locations, such that successful invasions would likely only develop from rare, and thus uncertain, new entries. In this context, a parameter governing susceptible host abundance could be nearly as important as one shaping the rate of spread.

In a final set of tests for each sensitivity scenario, we plotted the regions where introducing parametric uncertainty changed the mapped risk estimates considerably. We partitioned cells in the map of P_j for the baseline scenario into three broad classes, 'low', 'medium' and 'high' risk, corresponding to the intervals 0–0.25, 0.25–0.75 and 0.75–1, respectively. We then determined, for each sensitivity scenario, the percentage of the map area (i.e. the percentage of map cells) that moved from one risk class to another when compared with the baseline scenarios. These shifts can be portrayed in a classified map that highlights geographic locations with considerable changes in infestation risk. This classified map can also be used to determine if any geographic regions remained largely unchanged despite the introduction of parametric uncertainty at a specified level. Note that our choice of

breakpoints for these risk classes was arbitrary. Certainly, other analysts might find different sets of breakpoints more meaningful or opt to use more than three risk classes. The tests described here should remain applicable, regardless of such choices.

Table 13.2 shows the percentages of the map area that shifted from one risk class to another in one-parameter-at-a-time sensitivity scenarios. Results are displayed for scenarios at small (±10%), moderate (±25%) and high (±40%) levels of introduced parametric uncertainty. At ±10% uncertainty, the sensitivity scenarios typically exhibited only modest shifts in risk class (i.e. <5% of the map area relative to the baseline scenario), except for the local probability of entry, $W_{x(t)}$, which showed a relatively large shift of 8.3% of the map area between the medium and low risk classes. We believe this shift is a consequence of the phenomenon we noted previously: added variability in $W_{x(t)}$ caused more invasion nuclei to enter geographically remote portions of our study area through time, increasing the invasion risk, P_j, but stabilizing the output uncertainty, $\sigma(P_j)$. This phenomenon likely explains similar shifts between medium and low risk for $W_{x(t)}$ (8.1% of the map area) and between high and medium risk for p_0 (8.1%) at ±40% uncertainty, as well as many of the other observed changes in risk class due to introduced parametric uncertainty. The greatest map-area shifts occurred with $d_{\max}$, which exhibited 17.4% and 27.7% shifts from high to medium risk at ±25% and ±40% uncertainty, respectively. In addition, the results for $d_{\max}$ from the full sequence of one-at-a-time sensitivity scenarios (Table 13.3) show a 9.8% map-area shift between high and medium risk at ±15% uncertainty. This is larger than any shift observed for the other five parameters, at any variability bound increment. There was also an 8.1% map-area shift between medium and low risk at ±15% uncertainty for $d_{\max}$.

The geographic distribution of these shifts is important. Figure 13.5 (see colour plate section) shows risk-class shifts for eastern North America for the scenarios with ±15% and ±50% uncertainty in $d_{\max}$. At ±15% uncertainty (Fig. 13.5a), most areas within the main invasion front at the 30-year time horizon (see Fig. 13.1 and the earlier description of the baseline scenario results) did not exhibit a change in risk class, although clusters of map cells with

Table 13.2. The percentage of the map area shifting from one risk class to another when varying one parameter at a time within three different symmetric uniform ranges: ±10%, ±25% and ± 40%. Percentages are relative to the class area totals for the baseline scenario.

Shift in risk class	Model parameter					
	$W_{x(t)}$	k	$d_{\max}$	p_0	s_v	g_v
10% added parametric uncertainty						
Low → medium[a]	0.5	4.3	3.0	1.0	1.3	1.7
Medium → low	8.3	1.2	3.5	5.4	4.4	2.6
High → medium	1.0	0.9	4.9	1.1	1.0	0.9
Medium → high	0.7	0.6	0.2	0.6	0.5	0.8
25% added parametric uncertainty						
Low → medium	2.2	2.8	3.5	2.3	2.6	2.5
Medium → low	1.7	1.3	6.6	2.0	1.6	3.7
High → medium	1.3	1.0	17.4	4.6	1.1	0.9
Medium → high	0.6	0.7	0.1	0.2	0.7	0.6
40% added parametric uncertainty						
Low → medium	0.6	3.7	4.4	1.4	2.1	5.8
Medium → low	8.1	2.2	5.7	5.5	3.5	1.1
High → medium	1.2	1.3	27.7	8.1	1.1	1.1
Medium → high	0.6	0.6	0.0	0.1	0.6	0.6

[a]Low risk, $P_j < 0.25$; medium risk, $0.25 \leq P_j \leq 0.75$, high risk: $P_j > 0.75$.

Table 13.3. The percentage of total map area shifting from one risk class to another when varying only the d_{max} parameter. Reported percentages are relative to the class area totals for the baseline scenario.

	Uniform variation of d_{max}, percentage of the baseline value								
Shift in risk class	±5%	±10%	±15%	±20%	±25%	±30%	±35%	±40%	±50%
Low → medium[a]	1.6	3.0	2.9	3.5	3.5	3.4	4.1	4.4	6.4
Medium → low	3.8	3.5	8.1	7.4	6.6	5.1	4.8	5.7	7.8
High → medium	3.4	4.9	9.8	12.1	17.4	20.6	25.2	27.7	34.9
Medium → high (×10)	2.8	2.2	1.3	1.1	0.8	0.8	0.4	0.3	0.3

[a]Low risk, $P_j < 0.25$; medium risk, $0.25 \leq P_j \leq 0.75$; high risk, $P_j > 0.75$.

high-to-medium risk shifts did appear near the front's southern and north-western edges. In the south-eastern USA, beyond the main front, shifts from medium to low risk, and vice versa, occurred primarily in coastal areas. This result likely reflects a high degree of variability in the patterns of expansion of new *S. noctilio* entries at the region's marine ports under an uncertain d_{max}, despite the fact that the region is relatively host-rich. Similar geographic patterns occurred at ±50% uncertainty (Fig. 13.5b), although more map cells were affected. Still, even at this high level of uncertainty in d_{max}, sizeable areas within and beyond the main invasion front did not display a change in risk class. In short, across much of eastern North America, the risk estimates appeared to be fairly robust to uncertainty in this highly influential parameter.

Conclusions

What did we learn about our *S. noctilio* invasion model from these analyses? Foremost, the sequence of sensitivity scenarios demonstrated that the maximum annual spread distance, d_{max}, was the most sensitive of the tested model parameters, followed to a somewhat lesser degree by p_0, the local dispersal probability. In hindsight, this result is unsurprising, since for many mechanistic models of invasion processes, model aspects governing dispersal, particularly long-distance dispersal, are the most influential and uncertain. (Parameters related to the invader's demography may also be influential and uncertain; see Neubert and Caswell, 2000 and Buckley *et al*., 2005.) Indeed, were this or a similar modelling approach applied to another invasive pest, we could expect dispersal to figure prominently in subsequent sensitivity analyses. Of course, the results for those other models and species of interest may not be as obvious as seen here. Those results would depend substantially on the amount of interplay between the model parameters given the specific circumstances (e.g. region of interest, dispersal behaviour and population dynamics) being modelled. In our case, we modelled an invasive alien pest that is a strong flier and has hosts that are widely distributed and fairly abundant in the region of concern; hence, minimal functional connectivity between host areas may be necessary for range expansion (Minor *et al*., 2009; Vogt *et al*., 2009). Another species may be more constrained in a practical sense by the geographic distribution of its host(s), so uncertainty in this constrained distribution (i.e. in host-related model parameters) could have a significant impact on model projections. Nevertheless, we believe that the small suite of tests and metrics we outlined here should facilitate similar model-based analyses of invasion risks and uncertainties, even if the results end up being somewhat ambiguous. We attempted to develop a toolbox that provides analysts with a capacity to measure uncertainty quantitatively and to portray those results geographically. We believe the spatial assessment of models for alien species is critical because invasions unquestionably play out over time and space.

A particular finding of our study is that with the addition of a small degree of uncertainty for the d_{max} parameter (i.e. ±15%), a sizeable proportion of the map area displayed a drop in risk class, either from high to medium or from medium to low. Small uncertainty effects have critical implications were we to use the *S. noctilio* model to portray the forecasted invasion risks to decision makers. The most important implication is that risk estimates from the model must be interpreted cautiously, because we do not have to be very wrong about our primary dispersal assumptions before we may begin to misestimate the invasion risk, which could lead to incorrect risk management decisions. Fortunately, other model parameters that we tested only begin to affect model results when the level of uncertainty is high. We can be more confident that our risk projections are reasonably robust to uncertainty in these parameters (although see discussion below regarding the possibility of severe parametric uncertainties).

Given the known sensitivity of the model to estimates of d_{max}, how might we best proceed operationally? Two possible directions emerge from these findings. First, as Fig. 13.5 (see colour plate section) suggests, even when d_{max} is treated as highly uncertain (±50%), the risk estimates for much of the study area are fairly robust (i.e. no appreciable change occurs in the coarse, high-, medium- or low-risk rankings). In turn, these unchanged portions of the map could probably be used confidently for some decision-making tasks, such as prioritizing locations for the allocation of resources for monitoring and/or management.

Nevertheless, a decision maker may be reluctant to use a risk map if a significant portion of it has apparently been compromised by uncertainty. This predilection may just be a matter of decision makers' personal discretion or, more precisely, her or his degree of aversion to uncertainty. We accept this line of thinking. If this is the case, the sensitivity results suggest a second direction in which to proceed: determining how to resolve the lack of information about dispersal. This information gap could probably be achieved through additional research on important dispersal mechanisms of the pest of interest. Indeed, this is one of the reasons why our own research has increasingly focused on dispersal mechanisms related to human-mediated, long-distance dispersal – such as international and domestic trade (Koch *et al*., 2011; Yemshanov *et al*., 2012) – which are widely acknowledged as being pivotal to biological invasions yet poorly characterized. Alternatively, the dispersal modelling component for the pest of interest might also be improved via field study of its dispersal behaviour. For instance, now that *S. noctilio* is established in eastern North America, it might be possible to develop an appropriate dispersal function based on the invasive populations rather than the more indirect source of distributional observations in its native or previously invaded range. If additional research is not feasible, further review of existing literature – perhaps with guidance from experts – might uncover a species that can serve as a reasonable, if imperfect, proxy for the pest of interest when defining dispersal or other model parameters (e.g. Venette and Cohen, 2006).

In any case, our study has demonstrated that the use of sensitivity analysis techniques can reveal important sources of uncertainty (i.e. parametric uncertainty in this case) in pest risk maps and their underlying models. Still, the approach remains limited in terms of its ability to diagnose when those uncertainties might start to alter decision-making priorities. For example, while we were able to quantify when uncertainty in d_{max} began to impact the *S. noctilio* model's output risk estimates, what if we were drastically wrong about one or more of our other parameter estimates? In fact, what if one of our parameter estimates was off by a factor of 10 or more? Consequently, evaluating the parameter in question at ±50% uncertainty might generate an undeservedly optimistic impression of its robustness to uncertainty. As a possible solution, an analyst might opt to implement sensitivity scenarios with much wider

uncertainty bounds (e.g. ±1000%), but for relatively fine-scale stochastic simulation models, the computation time required to complete a comprehensive analysis with very wide uncertainty bounds may make this an impractical option. This would be especially true if the analyst deemed it necessary to evaluate the sensitivity of a large number of model parameters. Sampling techniques such as Latin hypercube sampling could reduce the required number of replications (Helton and Davis, 2002; Xu *et al*., 2005) and thus the computation time. Yet, the best way to achieve efficiency in the face of possibly severe uncertainty may be to adopt the perspective that the impact of uncertainty is best evaluated in the context of a small set of discrete choices about how the model results will be implemented. For instance, if the results will be used to support a long-term surveillance scheme, it might be wise to lay out a few different hypothetical surveillance schemes and perform a cursory examination of how each scheme responds to various amounts of introduced parametric uncertainty. At the least, working from this perspective might help the analyst narrow down the model parameters that require particular focus, and the uncertainty bounds that should be implemented, in order to identify the most robust choice.

Ultimately, we would like to see sensitivity-based analyses of uncertainty become standard practice in pest risk modelling and mapping. Despite limitations with the approach, it can be instructive to analysts when judging the value of their outputs for decision support. For example, maps depicting shifts in risk class at various levels of added uncertainty (such as in Fig. 13.5; see colour plate section) may be paired with the 'baseline scenario' risk map outputs to communicate the potential impact of parametric uncertainty for decision making. Furthermore, while the approach does not facilitate direct incorporation of measured uncertainties into output risk products, it might possibly be used in concert with other analytical approaches that do provide this option (see Yemshanov *et al*., Chapter 14 in this volume).

This chapter is enhanced with supplementary resources.

To access the material please visit:

www.cabi.org/openresources/43946/

References

Andrews, C.J., Hassenzahl, D.M. and Johnson, B.B. (2004) Accommodating uncertainty in comparative risk. *Risk Analysis* 24, 1323–1335.

Ben-Haim, Y. (2006) *Info-Gap Decision Theory: Decisions Under Severe Uncertainty*, 2nd edn. Academic Press, Waltham, Massachusetts.

Borchert, D., Fowler, G. and Jackson, L. (2007) *Organism Pest Risk Analysis: Risks to the Conterminous United States Associated with the Woodwasp,* Sirex noctilio *Fabricius, and the Symbiotic Fungus,* Amylostereum areolatum *(Fries: Fries) Boidin*. US Department of Agriculture, Animal and Plant Health Inspection Service, Plant Protection and Quarantine, Center for Plant Health Science and Technology, Plant Epidemiology and Risk Analysis Laboratory, Raleigh, North Carolina.

Buckley, Y.M., Brockerhoff, E., Langer, L., Ledgard, N., North, H. and Rees, M. (2005) Slowing down a pine invasion despite uncertainty in demography and dispersal. *Journal of Applied Ecology* 42, 1020–1030.

Carnegie, A.J., Matzuki, M., Haugen, D.A., Hurley, B.P., Ahumada, R., Klasmer, P., Sun, J. and Iede, E.T. (2006) Predicting the potential distribution of *Sirex noctilio* (Hymenoptera: Siricidae), a significant exotic pest of *Pinus* plantations. *Annals of Forest Science* 63, 119–128.

Cook, A., Marion, G., Butler, A. and Gibson, G. (2007) Bayesian inference for the spatio-temporal invasion of alien species. *Bulletin of Mathematical Biology* 69, 2005–2025.

Corley, J.C., Villacide, J.M. and Bruzzone, O.A. (2007) Spatial dynamics of a *Sirex noctilio* woodwasp population within a pine plantation in Patagonia, Argentina. *Entomologia Experimentalis et Applicata* 125, 231–236.

Crosetto, M. and Tarantola, S. (2001) Uncertainty and sensitivity analysis: tools for GIS-based model implementation. *International Journal of Geographical Information Science* 15, 415–437.

Crosetto, M., Tarantola, S. and Saltelli, A. (2000) Sensitivity and uncertainty analysis in spatial modelling based on GIS. *Agriculture, Ecosystems & Environment* 81, 71–79.

de Groot, P., Nystrom, K. and Scarr, T. (2006) Discovery of *Sirex noctilio* (Hymenoptera: Siricidae) in Ontario, Canada. *The Great Lakes Entomologist* 39, 49–53.

Dodds, K.J., Cooke, R.R. and Gilmore, D.W. (2007) Silvicultural options to reduce pine susceptibility to attack by a newly detected invasive species, *Sirex noctilio*. *Northern Journal of Applied Forestry* 24, 165–167.

Dodds, K.J., de Groot, P. and Orwig, D.A. (2010) The impact of *Sirex noctilio* in *Pinus resinosa* and *Pinus sylvestris* stands in New York and Ontario. *Canadian Journal of Forest Research* 40, 212–223.

Elith, J., Burgman, M.A. and Regan, H.M. (2002) Mapping epistemic uncertainties and vague concepts in predictions of species distribution. *Ecological Modelling* 157, 313–329.

Frey, H.C. and Patil, S.R. (2002) Identification and review of sensitivity analysis methods. *Risk Analysis* 22, 553–578.

Fuentes, M.A. and Kuperman, M.N. (1999) Cellular automata and epidemiological models with spatial dependence. *Physica A* 237, 471–486.

Gibson, G.J. and Austin, E.J. (1996) Fitting and testing stochastic models with application in plant epidemiology. *Plant Pathology* 45, 172–184.

Helton, J.C. and Davis, F.J. (2002) Illustration of sampling-based methods for uncertainty and sensitivity analysis. *Risk Analysis* 22, 591–622.

Helton, J.C., Johnson, J.D., Sallaberry, C.J. and Storlie, C.B. (2006) Survey of sampling-based methods for uncertainty and sensitivity analysis. *Reliability Engineering and System Safety* 91, 1175–1209.

Hoebeke, E.R., Haugen, D.A. and Haack, R.A. (2005) *Sirex noctilio*: discovery of a palearctic siricid woodwasp in New York. *Newsletter of the Michigan Entomological Society* 50, 24–25.

Koch, F.H., Yemshanov, D., McKenney, D.W. and Smith, W.D. (2009) Evaluating critical uncertainty thresholds in a spatial model of forest pest invasion risk. *Risk Analysis* 29, 1227–1241.

Koch, F.H., Yemshanov, D., Colunga-Garcia, M., Magarey, R.D. and Smith, W.D. (2011) Potential establishment of alien-invasive forest insect species in the United States: where and how many? *Biological Invasions* 13, 969–985.

Li, H. and Wu, J. (2006) Uncertainty analysis in ecological studies: an overview. In: Wu, J., Jones, K.B., Li, H. and Loucks, O.L. (eds) *Scaling and Uncertainty Analysis in Ecology: Methods and Applications*. Springer, Dordrecht, The Netherlands, pp. 43–64.

MacKay, D.J.C. (2003) *Information Theory, Inference, and Learning Algorithms*. Cambridge University Press, Cambridge.

Minor, E.S., Tessel, S.M., Engelhardt, K.A.M. and Lookingbill, T.R. (2009) The role of landscape connectivity in assembling exotic plant communities: a network analysis. *Ecology* 90, 1802–1809.

Morgan, M.G. and Henrion, M. (1990) *Uncertainty: A Guide to Dealing with Uncertainty in Quantitative Risk and Policy Analysis*. Cambridge University Press, New York.

National Agricultural Pest Information System (2013) *Survey Status of Sirex Woodwasp* – Sirex noctilio *(All Years)*. US Department of Agriculture, Animal and Plant Health Inspection Service, Plant Protection and Quarantine (USDA-APHIS-PPQ) and Purdue University, West Lafayette, Indiana. Available at: http://pest.ceris.purdue.edu/map.php?code=ISBBADA&year=alltime (accessed 22 December 2013).

Neubert, M.G. and Caswell, H. (2000) Demography and dispersal: calculation and sensitivity analysis of invasion speed for structured populations. *Ecology* 81, 1613–1628.

Rafoss, T. (2003) Spatial stochastic simulation offers potential as a quantitative method for pest risk analysis. *Risk Analysis* 23, 651–661.

Refsgaard, J.C., van der Sluijs, J.P., Højberg, A.L. and Vanrolleghem, P.A. (2007) Uncertainty in the environmental modelling process – a framework and guidance. *Environmental Modelling & Software* 22, 1543–1556.

Regan, H.M., Colyvan, M. and Burgman, M.A. (2002) A taxonomy and treatment of uncertainty for ecology and conservation biology. *Ecological Applications* 12, 618–628.

Rossi, R.E., Borth, P.W. and Tollefson, J.J. (1993) Stochastic simulation for characterizing ecological spatial patterns and appraising risk. *Ecological Applications* 3, 719–735.

Venette, R.C. and Cohen, S.D. (2006) Potential climatic suitability for establishment of *Phytophthora ramorum* within the contiguous United States. *Forest Ecology and Management* 231, 18–26.

Vogt, P., Ferrari, J.R., Lookingbill, T.R., Gardner, R.H., Riitters, K.H. and Ostapowicz, K. (2009) Mapping functional connectivity. *Ecological Indicators* 9, 64–71.

Walker, W.E., Harramoës, P., Rotmans, J., van der Sluijs, J.P., van Asselt, M.B.A., Janssen, P. and Krayer von Krauss, M.P. (2003) Defining uncertainty – a conceptual basis for uncertainty management in model-based decision support. *Integrated Assessment* 4, 5–17.

Xu, C., He, H.S., Hu, Y., Chang, Y., Li, X. and Bu, R. (2005) Latin hypercube sampling and geostatistical modeling of spatial uncertainty in a spatially explicit forest landscape model simulation. *Ecological Modelling* 185, 255–269.

Yamada, K., Elith, J., McCarthy, M. and Zerger, A. (2003) Eliciting and integrating expert knowledge for wildlife habitat modelling. *Ecological Modelling* 165, 251–264.

Yemshanov, D., Koch, F.H., McKenney, D.W., Downing, M.C. and Sapio, F. (2009a) Mapping invasive species risks with stochastic models: a cross-border US–Canada application for *Sirex noctilio* Fabricius. *Risk Analysis* 29, 868–884.

Yemshanov, D., McKenney, D.W., De Groot, P., Haugen, D.A., Sidders, D. and Joss, B. (2009b) A bioeconomic approach to assess the impact of an alien invasive insect on timber supply and harvests: a case study with *Sirex noctilio* in eastern Canada. *Canadian Journal of Forest Research* 39, 154–168.

Yemshanov, D., McKenney, D.W., Pedlar, J.H., Koch, F.H. and Cook, D. (2009c) Towards an integrated approach to modelling the risks and impacts of invasive forest species. *Environmental Reviews* 17, 163–178.

Yemshanov, D., Koch, F.H., Ducey, M. and Koehler, K. (2012) Trade-associated pathways of alien forest insect entries in Canada. *Biological Invasions* 14, 797–812.